

FIELD EMISSION SIMULATION FOR KEK-ERL 9-CELL SUPERCONDUCTING CAVITY

Enrico Cenni[#]

The Graduate University for Advanced Studies, KEK, Tsukuba, Ibaraki, Japan
 Takaaki Furuya, Hiroshi Sakai, Kensei Umemori, Kenji Shinoe, Masato Satoh
 KEK, Tsukuba, Ibaraki, Japan
 Masaru Sawamura
 JAEA, Tokai, Naka, Ibaraki, Japan

Abstract

In order to develop the Energy Recovery Linac at KEK, we are studying the performance of L-band superconducting cavities by means of vertical tests. One of the limiting factor for the cavities performance is the power losses due to field emitted electrons. To account with this phenomena, a particle tracking code is used to study electron trajectories and deposited energy on the inner surface of the cavity. Different emitter locations were tested within a range of accelerating fields and phases in order to reproduce different scenario. The final goal of this study is to locate the sources of the electrons inside the cavity through a deeper understanding of the phenomena.

INTRODUCTION

At KEK a compact ERL (cERL) is now under construction, to demonstrate the performance of components under CW operation at 100 mA of currents, 3GeV of energy and with ultra-short pulses of 100 fs.

Field emitted electrons are a key issue for the cavity performance, accelerated electrons increase the cavity losses and can generate dark current through the accelerating structure specially for CW operation. Our group has developed and characterized the superconductive cavities for the main accelerator section, figure 1 shows the SRF cavity for cERL. The performances of two L-band 9-cell superconductive cavities were studied by means of vertical tests after different surface treatment [1]. In order to obtain a precise diagnosis of the cavities during the tests we have used a rotating mapping system equipped with X-ray sensors (PIN diodes) and temperature sensors (carbon resistors). A more detailed description of the setup is available in reference [2]. The data gathered during vertical test were analysed and compared to simulation results to understand field emission dynamics.

CAVITIES

Two 1.3GHz superconductive cavities have been manufactured following the design for the main acceleration section of the ERL project. The main cavity parameters are summarized in Table 1.



Figure 1: KEK-ERL model-2.

Table 1: Parameters for KEK-ERL model-2 cavity

| | | | |
|--------------------|--------------|--------------------|---------------|
| Frequency | 1.3GHz | Coupling | 3.8 % |
| R_{sh}/Q | 897 Ω | Geom.Fac. | 289 Ω |
| E_{peak}/E_{acc} | 3.0 | H_{peak}/E_{acc} | 42.5Oe/(MV/m) |

SIMULATION

Trajectories Calculation

The code used for electron tracking was originally designed to track electrons for multipacting analysis (FishPact[3]). The code has been modified in order to obtain information concerning field emitted electrons, by means of accelerating field, impact location, energy, impact angle and emission phase for the cERL model-2 cavity. The trajectories were calculated integrating the relativistic equation of motion using the 4th order Runge-Kutta method until the electrons hit the cavity walls. The results were crosschecked with CST Particle Studio® suite.

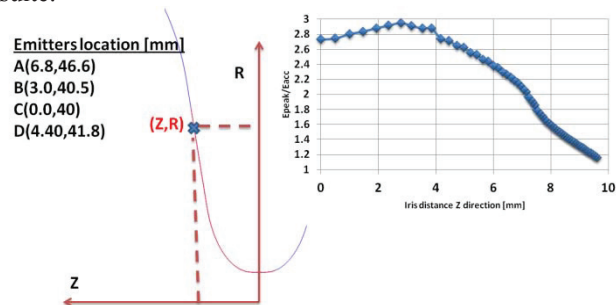


Figure 2: (left) Definition of the emitter coordinates Z coordinates along the cavity axis and R coordinates along radial axis, (right) E_{peak}/E_{acc} with respect to Z coordinate.

[#]enrico@post.kek.jp

In the simulation electrons were emitted perpendicular to the metal surface with an energy of 2eV from each emitters. The emitter locations are defined as shown in figure 2. They can be emitted during different RF phase and accelerating field, also the emitter position can be decided along the cavity surface. Once the electron hit the cavity wall the impact energy, location and angle were recorded along with all the information concerning the emission condition (Eacc, phase, position).

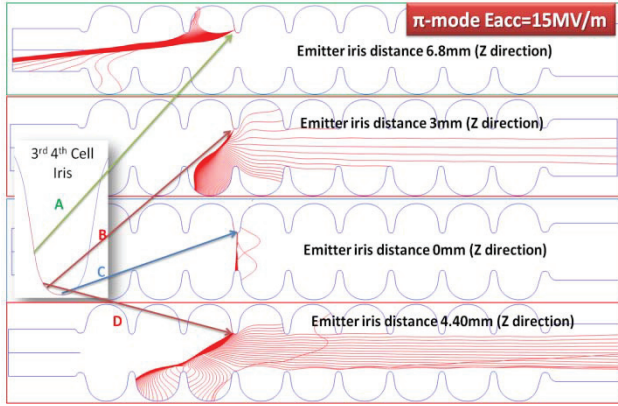


Figure 3: Trajectories from different emitters and RF phases at $E_{acc}=15MV/m$.

Figure 3 shows trajectories generated by emitters located at different distance from the iris centre. It could be notice how the impact location change with respect to the RF phase and with respect to the emitter position. Trajectories that start from the iris centre mainly land on the opposite iris wall, while for emitters located away from the iris centre emitted electrons have some chance to exit the cavity. Emitter B and D both have many trajectories that can reach one end of the cavity, but as will be shown in the next section the power loss (or energy deposited on the cavity walls) are different.

Emitted Current Density and Impact Energy

According to the Fowler-Nordheim (FN) equation, the electron current density depends on few parameters

$$J = \frac{A_{FN}(\beta_{FN}E_{surf}(t))^2}{\varphi} e^{\frac{-B_{FN}\varphi^{1.5}}{(\beta_{FN}E_{surf}(t))}} \left[\frac{A}{m^2} \right]$$

where J is the current density, E_{surf} is the electric field on the surface in V/m, φ is the Niobium working function which equals to 4.3eV, β_{FN} is the field enhancing factor due to the emitter asperity, A_{FN} and B_{FN} are two constants respectively equal to $1.54 \cdot 10^{-6}$ and $6.83 \cdot 10^9$.

Due to oscillation of the electro-magnetic field also the emitted current change with time and if a sine function dependency on time (or RF phase θ) is assumed the current density is like shown in figure 4.

It can be noticed that the current density is approximately a Gaussian with respect to the RF phase with a

$\sigma_{\theta} \sim \sqrt{(\beta_{FN}E_{surf}(\frac{\pi}{2})) / B_{FN}\varphi^{1.5}}$, if a maximum surface field between 45 and 75MV/m is considered with $\beta_{FN}=100$ then σ_{θ} span from 16° to 20° and the maximum

located at 90° of RF phase. In the calculation made in this paper β_{FN} will be always considered equal to 100.

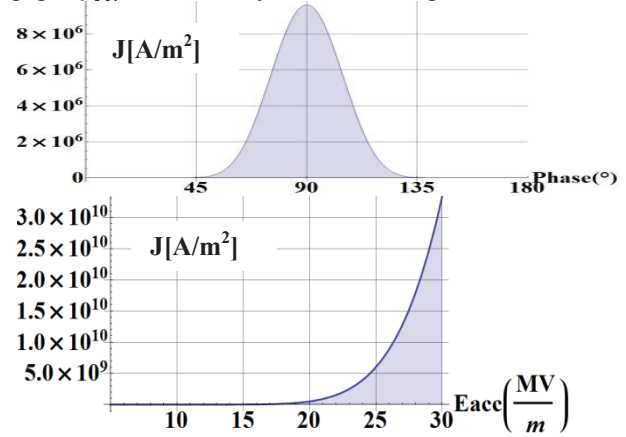


Figure 4: (above) Current density with respect to RF phase assuming, $E_{surf}=45MV/m$ and $\beta_{FN}=100$, (below) current density with respect to Eacc.

Figure 5 shows a result using an emitter located near the iris between the 3rd and 4th cell. Trajectories for different RF phases are represented on the left part of the figure. The plot represents the impact energy (in blue) and the product between impact energy and emitted current density (in green). The data are collected for an accelerating field of 15MV/m and $\beta_{FN}=100$.

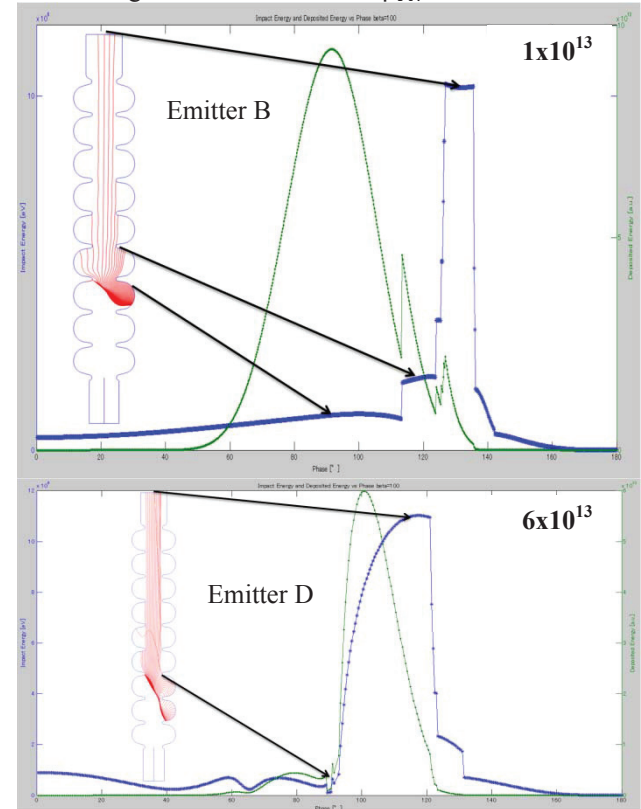


Figure 5: Impact energy (blue curve) and the product between emitted current density and impact energy (green curve) with respect to emission RF phase, emitter is located on iris between 3rd and 4th cell, the accelerating field is 15MV/m. In the left part are shown the trajectories inside the cavity.

Copyright © 2012 by IEEE - cc Creative Commons Attribution 3.0 (CC BY 3.0) - cc Creative Commons Attribution 3.0 (CC BY 3.0)

While the trajectories that exit the cavity bring a small current density they still have greater impact energy than the others. The product of the two gives the peaks on the green curve. This quantity is proportional to the power loss due to the field emitted current or the power deposited on the cavity surface upon electrons impact. It could be noticed how the RF phase offset between the current density peak (located at 90°) and the impact energy peak influence the product of the quantity. While emitter B and D both have trajectories that can reach one end of the cavity, in the latter case the product is 6 times bigger. This is the reason why it is so important to know which emitter locations can produce the bigger power loss.

RESULTS AND DISCUSSION

In order to understand which area around the iris could be more dangerous, in terms of power loss, a region of 30mm was checked by placing 1 emitter every 0.5mm. Here are presented the results obtained from emitters located on the iris between the 3rd and the 4th cell.

Figure 6 represents a contour plot of the E_{surf}/E_{acc} at different RF phases, the green and the red crosses are the emitter locations that produce some trajectories that can exit the cavity with a specific RF phase. The coloured lines represent the emitter locations shown in Figure 3.

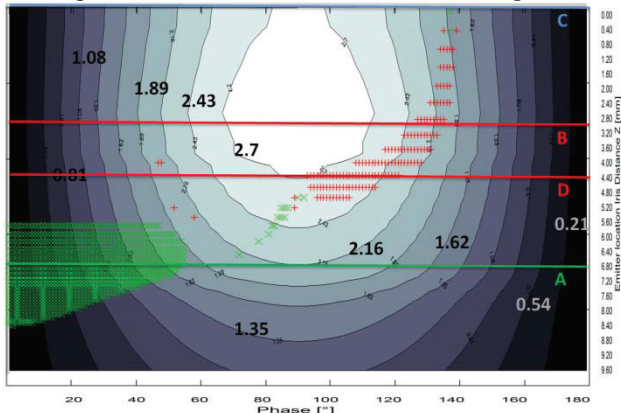


Figure 6: Contour plot of E_{surf}/E_{acc} on x-axis there are RF phases on y-axis the distance from Iris (Z coordinate) surface red and green crosses are emitter locations, with respect to RF phase, that can produce a trajectory that exit the cavity.

The impact energy with respect to the emitter locations and RF emission phase with an accelerating field of 15MV/m is represented on Figure 7. The bright area corresponds to trajectories that have a greater impact energy. The product of the emitted current density and impact energy with respect to the emitters location and emission RF phase is represented on Figure 8. The bright area corresponds to a region near the iris, as shown in the box of figure 8, with an approximate length of 5mm, an emitter located in this region can produce a greater cavity loss than in other location.

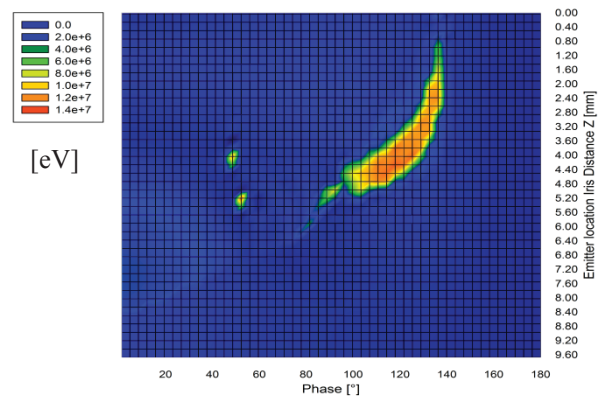


Figure 7: The impact energy [eV] is plotted with respect to emission RF phase (x axis) and emitters location (y axis) as distance from iris center on Z cavity coordinate.

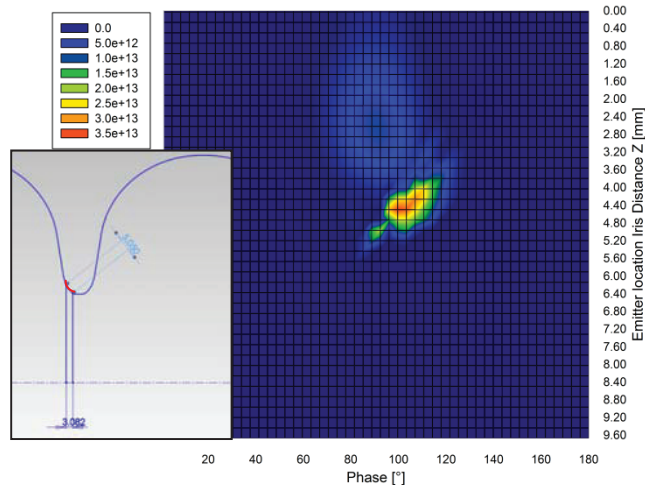


Figure 8: The product of impact energy and emitted current density is plotted with respect to emission RF phase (x axis) and emitters location (y axis) as distance from iris center on Z axis. In the left box the location of the bright area (“danger area”) on the iris.

Finally, these simulation results (obtained by FishPact) were compared for some specific cases with data obtained with CST Particle Studio. Both code are in a reasonable agreement.

SUMMARY

This study has shown that by using a particle tracking code it is possible to locate regions where emitters can produce a greater cavity loss or greater energy deposition on the cavity walls. To locate those area on the iris, information such as emitter locations, emission RF phase, impact energy, β_{FN} and surface electric field were necessary. Those data were collected through simulation and analysis codes in order to investigate the complex relationship between field emission and cavity working condition.

REFERENCES

- [1] K. Umemori et al., in these proceedings.
- [2] H. Sakai et al., Proc. of IPAC10, p2950.
- [3] FishPact, <http://code.google.com/p/fishpact/>